www.verizonaonlinepublishing.com
Vol: 2, Issue: 1

VERIZONA PUBLISHER
Publishing Your Ideas

Journal of Energy and Environmental Research and Technology

Software to Compensate Coincidence Losses in the Environmental Sample Analysis of a Digital Anti-Compton Spectrometer

Weihua Zhang*, **Kenneth Lam, Kurt Ungar and Chuanlei Liu**

Radiation Protection Bureau, Health Canada, 775 Brookfield Road, Ottawa, Ontario, Canada

***Corresponding author:** Weihua Zhang, Radiation Protection Bureau, Health Canada, 775 Brookfield Road, Ottawa, Ontario, Canada K1A 1C1; E mail: weihua.zhang@canada.ca

Article Type: Research, **Submission Date**: 08 May 2018, **Accepted Date:** 01 June 2018, **Published Date:** 04 July 2018.

Citation: Weihua Zhang, Kenneth Lam, Kurt Ungar and Chuanlei Liu (2018) Software to Compensate Coincidence Losses in the Environmental Sample Analysis of a Digital Anti-Compton Spectrometer. J Eng Env Resol 2(1): 1-8. Doi: https://doi.org/10.24218/jeert.2018.03

Abstract

Anti-Compton spectroscopy is a useful approach to analyze low-level contaminants in environmental samples that would otherwise be obscured by the Compton signal of the natural radionuclides present in the sample matrix. An example of this is the sensitive identification of ^{137}Cs in soil samples. A challenge of the anti-Compton technique is that the anti-coincidence veto to remove Compton scattered photons also suppresses the identification of contaminant radionuclides that have cascade gamma emissions such as ^{60}Co. This is a major limitation of the technique in environmental sample analysis. The time stamped pulse analysis method presented in this paper recovers the undesired full-energy-peak (FEP) coincidence losses for cascade radionuclides that trigger the anti-Compton spectrometer veto while retains suppression of true Compton events to keep the improved detection limit, thus extending the usefulness of the anti-Compton spectroscopy. In this study, the software has been used to analyse the radionuclides with a relative simple decay scheme, such as ^{22}Na, ^{60}Co and ^{88}Y, and a complex decay scheme, such as ^{125}Sb, ^{134}Cs, ^{152}Eu and ^{154}Eu. The results have indicated that in the reconstruct anticoincidence spectra the FEP restoration efficiency, both for minor and major peaks, is near 100%.

Introduction

To achieve low detection limits for environmental sample analysis, Compton continuum suppression gamma-ray spectrometer has been used for several decades. However, it has to be used with care for radionuclides with complex decay schemes such as ^{60}Co, ^{106}Rh, ^{110m}Ag, ^{124}Sb, ^{134}Cs, and ^{154}Eu. These types of radionuclides may emit many gamma-rays in coincidence. There is a possibility of two gamma-rays from the same disintegration being detected by both detectors at the same time. These events will be considered as Compton events and rejected, leading to undesired FEP cascade losses. The limitations of the spectroscopic performance not only reduce the sensitivity for determining these radionuclides, but also provide difficulties for quantifying the activity with a normal true FEP efficiency curve both for radionuclides with cascading gamma-rays and single-line gamma-ray emitters.

In order to recover the undesired FEP cascade losses, Zhang et al. [1] converted an Ortec Compton suppression system into a digital Compton suppression spectroscopy. Instead of using analog electronic pulses to determine the coincidence event, the waveform signals from the HPGe preamplifier, the PMTs of the NaI(Tl) annulus and the PMT of the NaI(Tl) plug detectors were fed into three different channels of a pixie-4 card (XIA LLC) for pulse-height and time coincidence measurement. The pixie-4 digitizer hardware controls triggering, pulse-height analysis, digitized pulse capture, coincidence logic, and live-time accounting. Each event is recorded together with a timestamp, channel number and energy (DSP-units) in a 4-column data file.

In this study, open source software with a new algorithm has been developed for offline analysis of the collected data results. The software allows one to select coincidence and anticoincidence events between the HPGe detector and the Na(Tl) annulus/plug guard detectors. This creates corresponding arrays and allows the user to build up both coincidence and anticoincidence spectra.

The new algorithm is then used to identify and select the undesired FEP cascade losses due to gamma-ray cascade decay in the coincidence spectrum. The undesired FEP cascade losses will be allowed to add back to anticoincidence spectrum for analysis. The idea behind this article is to present the new FEP cascade losses recovery algorithm developed in this study, and to show its applications on measurement of environmental aerosol samples containing the radionuclides of ^{134}Cs,^{60}Co and

^{22}Na with the digital anti-Compton spectrometer. The study also demonstrated successful applications of the algorithm to reconstruct anticoincidence spectra with more than 99% FEP efficiency restoration for the radionuclides, such as ^{154}Eu, ^{125}Sb and ^{152}Eu, with a complex decay scheme.

Anti-Compton spectrometer and the software architecture

The primary detector used in this study was an Ortec n-type GMX HPGe coaxial detector with a crystal diameter of 66.2 mm and a length of 69.0 mm. This detector has a peak-to-Compton plateau ratio of 52:1 for the 1332.5 keV peak of ^{60}Co, a relative efficiency of 54% with respect to the efficiency (counted at 25 cm) of a standard (3"×3") NaI(Tl) detector, and a warranted resolution (FWHM) of 2.53 keV at 1332.5 keV peak of ^{60}Co. The HPGe detector endcap was made entirely of carbon fiber to meet the high radiation transmission requirement. The guard detectors used in the system consisted of a 9″×9″ NaI(Tl) annulus (inner diameter 4.7”) with four photomultiplier tubes (PMTs) and a 3″×3″ NaI(Tl) plug with one PMT. According to the manufacturers specification, with anticoincidence counting mode, the peak-to-Compton plateau ratio of this system was 950:1 at the 661.7 keV peak of ^{137}Cs, using the IEEE convention for the number of counts per channel in the Compton plateau, as defined in ANS/IEEE Standard 325-1986 [2].

The data-acquisition system for the spectrometer utilizes all digital electronics based on the XIA LLC Digital Gamma Finder (DGF)/Pixie-4 software and card package. The same detectors described in the NIM electronics analog counting system were used. The pixie-4 card is a four channel digital pulse-processing module. The waveform signals from the preamplifier of the HPGe, PMTs of the NaI(Tl) annulus and plug detectors were fed into two different channels of the pixie-4 card for pulse height and time coincident measurement. The input signals from the PMT of NaI(Tl) have to be attenuated by adjusting the position of a jumper in the corresponding channel. At each channel, the input signals were continuously sampled and digitized by a 14-bit analog-to-digital converter (ADC). The signal pulse-height was determined to be 16-bit resolution by a programmable digital trapezoidal energy filter implemented in a field-programmable gate array (FPGA). Event timing and pulse-pileup inspection was also carried out in the FPGA by a fast programmable trapezoidal trigger filter. Events were time-stamped at the full ADC rate of 75 MHz. The time resolution is about 13.3 ns. Whenever a valid event was detected, a digital signal processor (DSP) read out the energy filter values. It was then recorded together with the timestamp, channel number, and energy (DSP-units) in a 4-column array for offline analysis [3].

The software was designed such that it can parse Pixie-4 DAT output files and classify detections into anticoincident/coincident events arrays, and to build up corresponding coincidence and anticoincidence spectrum. The lost Compton background events and FEP cascade coincidence losses in the anticoincidence array can be recorded in the coincidence spectrum as continue background and peaks. Using a Savitzky-Golay [4] digital filter to smooth the coincidence spectrum data, the peak regions were isolated using a second derivative criterion. The baseline was determined through the peak minima with a linear regression model. With the background counts subtracted, the coincidence peak counts were added back to the anticoincidence spectrum by channel to form a reconstructed anticoincidence spectrum with Compton suppression and minimized the FEP cascade coincidence losses.

The original anticoincidence and reconstructed anticoincidence spectral files were analysed by a software package named Unisampo/Shaman. Unisampo is gamma-ray spectrum analysis software [5]for peak energy and intensity determination, and Shaman is an expert system [6] for radionuclide identification and activity calculation. Shaman uses the peak quantitative analysis results from Unisampo together with a comprehensive nuclide library to explain each spectrum peak quantitatively. Its library has been tuned for the purposes of environmental radiation monitoring. Therefore, identification decisions made by the software reflect the environmental monitoring design criteria. In Shaman, algorithms have been implemented for coincidence summing corrections, which is important in close counting geometries and for complex decay schemes.

Results and discussion

Efficiency calibration

A mixed radionuclide air filter (50mm×4mm) puck source that is from National Physical Laboratory (NPL) and traceable to their primary standard was used for the HPGe detector efficiency calibration. The standard was measured by the anti-Compton spectrometer. The original anticoincidence and reconstructed anticoincidence spectra obtained by offline list-mode data process are illustrated in Figure 1. It is clear from Figure 1 that the FEP cascade losses at 898.8 keV(^{88}Y), 1173.2 keV and 1332.5 keV (^{60}Co)in the original anticoincidence spectrum have mostly been recorded in the coincidence spectrum. Thus, by searching through the coincidence spectrum, these FEP losses can be quantified and used to generate the reconstructed anticoincidence spectrum. The two spectra were both analysed by the Unisampo/Shaman package. The efficiency curves were calculated and are provided in Figure 2.

On the top of FEP cascade losses by anti-Compton counting there is another FEP loss caused by the true coincidence summing (TCS) in the HPGe detector. Its corrections have to be applied to 165.9 keV (^{139}Ce), 898.8 keV and 1836.1 keV (^{88}Y), and 1173.2 keV and 1332.5 keV (^{60}Co) peaks for efficiency calibrations. TCS occurs for radionuclides that emit two or more gamma rays in coincidence. The FEP losses by TCS are due to the sum of both photons when the coincident gamma rays or X-rays are captured within very short time interval compared to the charge collection time in the HPGe detector. These result in the signal lost in the FEP for the gamma rays and an increase in counts in the

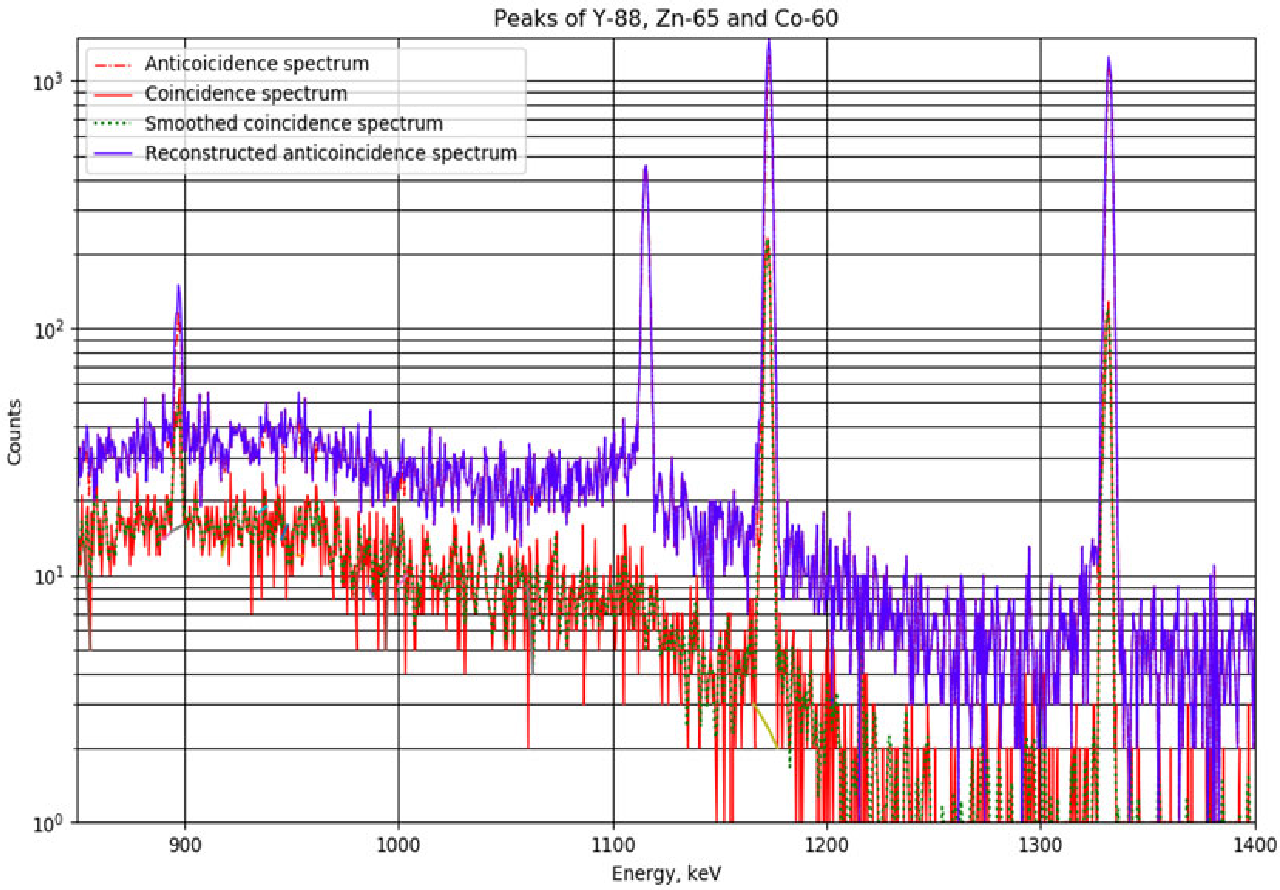

Figure 1: The standard calibration spectra (partial) to demonstrate the peak area recovery (at energy 898.8, 1173.2 and 1332.5 keV) by the reconstructed anticoincidence spectrum

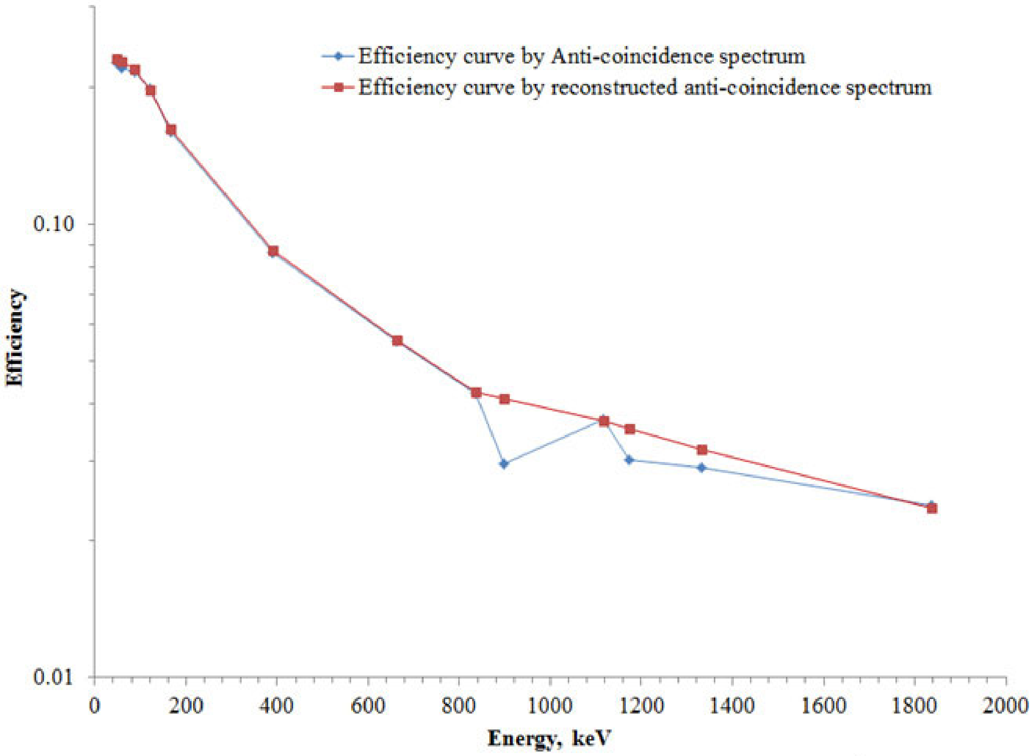

Figure 2: Efficiency calibration curves obtained by the mixed radionuclide standard using original anticoincidence and reconstructed anticoincidence spectra

spectrum background above the peaks as well as the appearance of peaks at the energy of the sum of the energies of the individual peaks. This kind of coincidence losses do not generate any coincidence peaks in the coincidence spectrum, thus cannot be corrected by this software. Figure 2 shows the plots of efficiency both corrected by the TCS correction factor as a function of energy. Here, practically all the points from monoenergetic sources are lying on the same curve. The efficiencies at 898.8 keV, 1173.2keV and 1332.5 keV, which were lying below the curve obtained by anticoincidence spectrum, are lying on the curve by reconstructed anticoincidence spectrum. This gives rise to a good efficiency curve after FEP cascade losses correction. Hence, it will be used for aerosol sample activity concentration analysis. It should also be noted that the efficiency at 1836.1 keV, which is out of the Compton suppression region of this spectrometer, is not influenced by FEP cascade losses by anti-Compton counting.

Aerosol sample analysis

Initial software testing was carried out with an aerosol sample by comparing the processed data with anti-Compton spectrometer to results obtained with a single HPGe detector. The aerosol sample is the reference sample prepared by the Eckert & Ziegler Analytics for laboratory proficiency test. The geometry of sample is the same as the mixed radionuclide standard used for efficiency calibration. Multi-line isotopes, such as ^{22}Na, ^{60}Co, ^{134}Cs, have been previously identified and quantified by the single HPGe

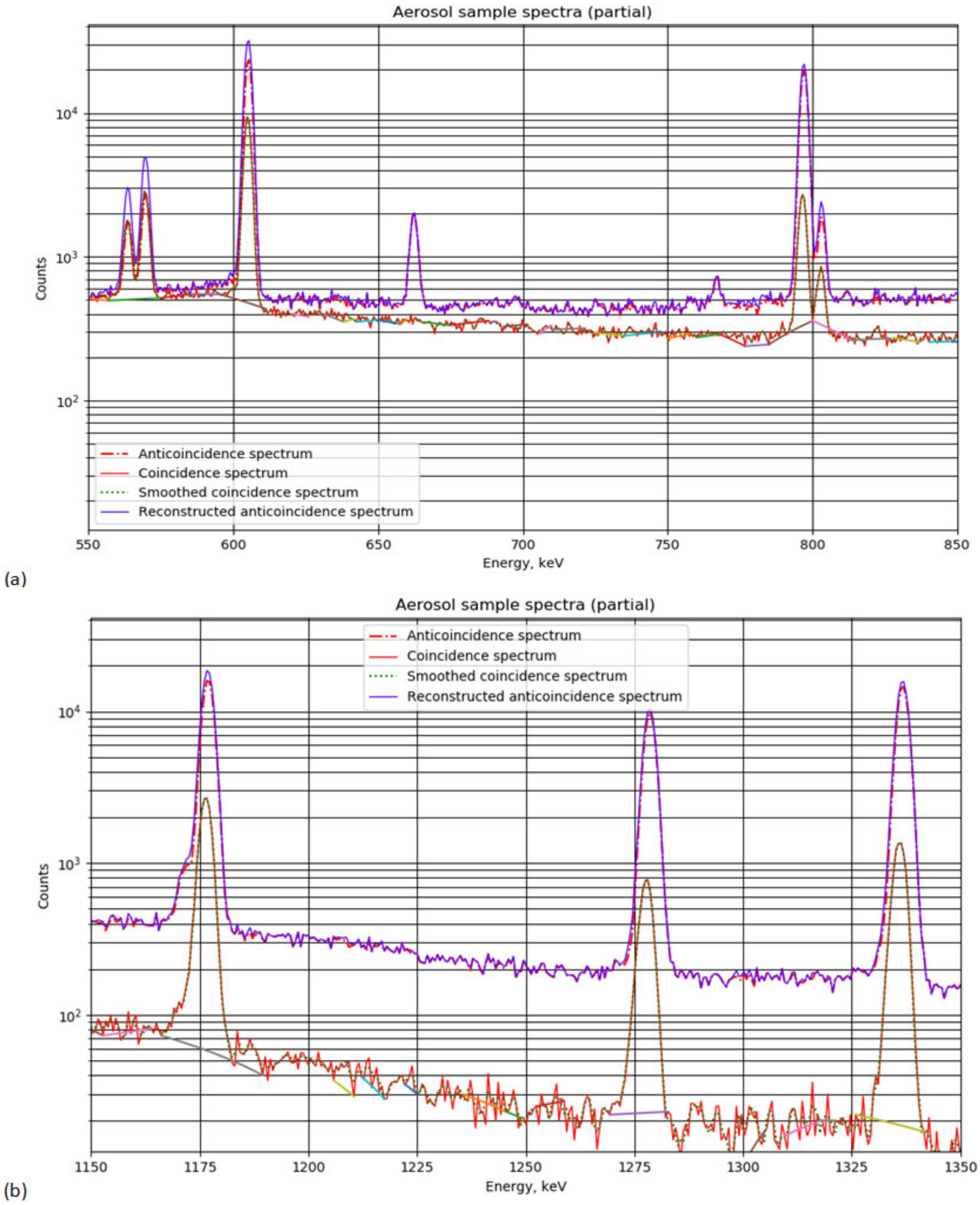

Figure 3: Comparison of anticoincidence, coincidence and reconstructed anticoincidence spectra collected by the aerosol sample for the energy range 550-850 keV (a) and 1150-1350 keV (b)

detector. The anticoincidence, coincidence and reconstructed anticoincidence spectra processed from offline list-mode data are illustrated in Figure 3. The analysed activity concentrations from the anticoincidence and reconstructed anticoincidence (both corrected by the same TCS correction factors) are presented in Table 1. As shown in Figure 3a, significant coincidence peaks, such as 563.2, 569.3, 604.7, 795.9, and 802.0 keV associated with^{134}Cs, have been observed. There is no coincidence peak at 661.7 keV, indicating the single-line isotope (^{137}Cs) has no FEP cascaded losses during anti-Compton counting. The Figure 3b shows well-defined coincidence peaks at 1274.5keV associated with ^{22}Na, and 1173.2, and 1332.5keV associated with ^{60}Co. The software developed in this study has successfully isolated these coincidence peaks and added coincidence peak counts back to the reconstructed anticoincidence spectrum.

Both anticoincidence and reconstructed anticoincidence spectra were analysed with the Unisampo/Shaman package using the efficiency curve mentioned above. The TCS correction factors, used for anticoincidence and reconstructed anticoincidence spectra analysis, were obtained by VGSL [7]. The activity concentrations obtained by the anticoincidence spectrum indicate that the effect of FEP cascade losses from the peaks is important in spectrum analysis for obtaining an unbiased activity for the radionuclides with complicated decay scheme. The FEP losses induced systematic errors reaching levels from several percent for ^{24}Na to more than several ten percent for ^{134}Cs, as shown in Table 1. The activity concentrations obtained by the reconstructed anticoincidence spectrum were in good agreement with those from the single HPGe measurement. The activity concentrations obtained by each gamma-ray peak associated to ^{60}Co and ^{134}Cs in the reconstructed anticoincidence spectrum also agreed well, which confirms that the software provides good compensation for the peaks with FEP cascade losses in anti-Compton counting.

More complicated cases

A multi-radionuclide standard source prepared by the Eckert & Ziegler Analytics was involved in the further testing of the software. The activities of ^{125}Sb, ^{154}Eu and ^{155}Eu were certified as reference values in this standard. The activity of ^{152}Eu (as impurity) was also given. Figure 4 shows the offline list-mode data processed anticoincidence, coincidence and reconstructed anticoincidence spectra by anti-Compton spectrometer. The analysis of the anticoincidence and reconstructed anticoincidence spectra for activity is presented in Table 2 along with the ratio to the reference value. As shown in Figure 4 (a, b, c, d), the spectra obtained by the standard was quite complex. The domninant peaks at 123.1, 247.9, 370.7, 591.8, 692.4, 723.3, 756.8, 873.2, 904.1, 996.3, 1004.7 keV from ^{154}Eu have been suppressed in the anticoincidence spectrum. The ^{154}Eu activities determined by these peaks in anticoincidence spectrum were reduced from 54% to 3% compared to the reference value, as shown in Table 2. On the other hand, the activities obtained by the same peaks with reconstructed anticoincidence spectrum were in good agreement with the reference value, which demonstrates that the software can compensate the loss of FEP counts for big peaks.

Significant FEP cascade losses can also be found for small peaks such as the peaks at 208.1 and 227.9 keV of ^{125}Sb and 344.3 and 411.1 keV of ^{152}Eu in the coincidence spectrum, (as shown in Figures 4b& c). The activity (determined by each individual peak) ratios to reference value are 0.62, 0.37, 0.75,

Table 1: Comparison between aerosol sample analysis results obtained by anticoincidence and reconstructed anticoincidence spectra using the same experimental efficiency curve of Figure 2 and TCS correction factors

			Activity concentrations (Bq/m^3) and ratios to the results by a single HPGe detector			
Radionuclide	Energy(keV)	TCS factor	By anticoincidence Spectrum		By reconstructed anticoincidence Spectrum	
^{22}Na	1274.5	1.56	3.17E-03	0.94	3.43E-03	1.02
^{60}Co	1173.2	1.17	2.89E-03	0.88	3.38E-03	1.03
^{60}Co	1332.5	1.20	3.08E-03	0.94	3.39E-03	1.03
^{134}Cs	475.4	1.52	2.00E-03	0.42	4.72E-03	0.98
^{134}Cs	563.2	1.60	2.43E-03	0.51	4.68E-03	0.98
^{134}Cs	569.3	1.57	2.35E-03	0.49	4.68E-03	0.98
^{134}Cs	604.7	1.31	3.47E-03	0.72	4.82E-03	1.01
^{134}Cs	795.9	1.24	4.14E-03	0.86	4.67E-03	0.98
^{134}Cs	802.0	1.52	3.45E-03	0.72	4.84E-03	1.01
^{134}Cs	1038.6	1.15	4.96E-03	1.04	4.95E-03	1.03
^{134}Cs	1168.0	0.70	3.95E-03	0.82	4.77E-03	1.00
^{134}Cs	1365.2	0.64	4.59E-03	0.96	4.69E-03	0.98
^{137}Cs	661.7	1.00	1.34E-04	0.98	1.36E-04	1.00
^{144}Ce	133.5	1.00	2.11E-03	1.04	2.12E-03	1.05
^{241}Am	59.5	1.00	4.92E-03	1.00	4.93E-03	1.00

Table 2: Comparison between the complex standard analysis results obtained by anticoincidence and reconstructed anticoincidence spectra, as shown in Figure 4

			Activity(Bq) and activity ratio to the reference value			
Radionuclide	**Energy(keV)**	**TCS factor**	**By anticoincidence Spectrum**		**By reconstructed anticoincidence Spectrum**	
^{154}Eu	123.1	1.93	6.19E+03	0.66	9.17E+03	0.97
^{154}Eu	247.9	1.98	4.36E+03	0.46	9.53E+03	1.01
^{154}Eu	370.7	0.69	4.95E+03	0.53	9.32E+03	0.99
^{154}Eu	591.8	1.66	6.48E+03	0.69	9.54E+03	1.01
^{154}Eu	692.4	1.62	8.00E+03	0.85	9.45E+03	1.00
^{154}Eu	723.3	1.45	7.47E+03	0.79	9.49E+03	1.01
^{154}Eu	756.8	1.73	8.93E+03	0.95	9.44E+03	1.00
^{154}Eu	873.2	1.56	8.63E+03	0.92	9.49E+03	1.01
^{154}Eu	904.1	1.54	8.75E+03	0.93	9.49E+03	1.01
^{154}Eu	996.3	1.09	8.68E+03	0.92	9.16E+03	0.97
^{154}Eu	1004.7	1.28	9.16E+03	0.97	9.27E+03	0.98
^{154}Eu	1128.6	0.17	9.14E+03	0.97	9.29E+03	0.99
^{154}Eu	1274.4	1.29	9.17E+03	0.97	9.18E+03	0.97
^{154}Eu	1397.5	1.27	9.23E+03	0.98	9.28E+03	0.98
^{154}Eu	1596.4	0.81	9.42E+03	1.00	9.47E+03	1.01
^{125}Sb	176.3	1.18	1.04E+04	1.03	1.05E+04	1.03
^{125}Sb	204.1	1.54	9.89E+03	0.97	1.05E+04	1.03
^{125}Sb	208.1	2.07	6.29E+03	0.62	1.03E+04	1.02
^{125}Sb	227.9	1.83	3.79E+03	0.37	1.04E+04	1.03
^{125}Sb	321.0	1.43	9.52E+03	0.94	1.01E+04	1.00
^{125}Sb	380.5	1.26	1.02E+04	1.00	1.01E+04	1.00
^{125}Sb	427.9	1.46	1.00E+04	0.99	9.98E+03	0.98
^{125}Sb	463.4	1.15	1.01E+04	1.00	1.00E+04	0.99
^{125}Sb	600.6	1.41	9.89E+03	0.98	9.87E+03	0.97
^{125}Sb	606.7	1.42	9.63E+03	0.95	9.71E+03	0.96
^{125}Sb	636.0	1.37	1.07E+04	1.05	1.05E+04	1.04
^{125}Sb	671.4	1.02	9.84E+03	0.97	9.69E+03	0.96
^{152}Eu	121.8	1.65	6.10E+02	0.98	6.32E+02	1.01
^{152}Eu	344.3	1.15	4.68E+02	0.75	6.34E+02	1.02
^{152}Eu	411.1	1.66	2.77E+02	0.44	6.38E+02	1.02
^{152}Eu	778.9	1.19	6.34E+02	1.01	6.36E+02	1.02
^{152}Eu	867.4	2.15	6.47E+02	1.04	6.36E+02	1.02
^{152}Eu	964.1	1.41	6.08E+02	0.97	6.08E+02	0.97
^{152}Eu	1085.9	0.96	6.11E+02	0.98	6.17E+02	0.99
^{152}Eu	1112.1	1.43	6.11E+02	0.98	6.20E+02	0.99
^{152}Eu	1213.0	1.49	6.19E+02	0.99	6.23E+02	1.00
^{152}Eu	1299.1	1.18	6.41E+02	1.03	6.23E+02	1.00
^{155}Eu	86.5	1.00	4.62E+03	1.01	4.58E+03	1.00
^{155}Eu	105.3	1.00	4.61E+03	1.01	4.56E+03	1.00

0.44 respectively, as shown in Table 2. The peak regions were successfully isolated to provide a near 100% peak recovery rate on these corresponding peaks by the software. As presented in Table 2, unbiased activities have been obtained by these for small peaks with the reconstructed anticoincidence spectrum. For other peaks at 204.1 and 321.0 keV of ^{125}Sb, the FEP cascade lossesdue to anti-Compton counting were less than 5%, as presented in Table 2. Only very small bumps can be seen in quite a noisy area, as shown in the coincidence spectrum of Figure 4. The software is still able to locate the peaks in a noisy data set, determine the baseline through the peak minima with a linear regression model, and recover the signal lost.

Conclusion

It has been demonstrated that the software, in its present form, has met the objective of facilitating routine acquisition of the digital anti-Compton spectrometer. By parsing list-mode data output files and classifying detections into anticoincident or coincident events, the software allows the simultaneous creation of coincidence and anticoincidence spectra from a single measurement. Using variants of peak detection algorithms, peaks in coincidence spectrum can be easily identified. Baseline models were created to build up reconstructed anticoincidence spectrum which provides a near 100% FEP recovery rate for the

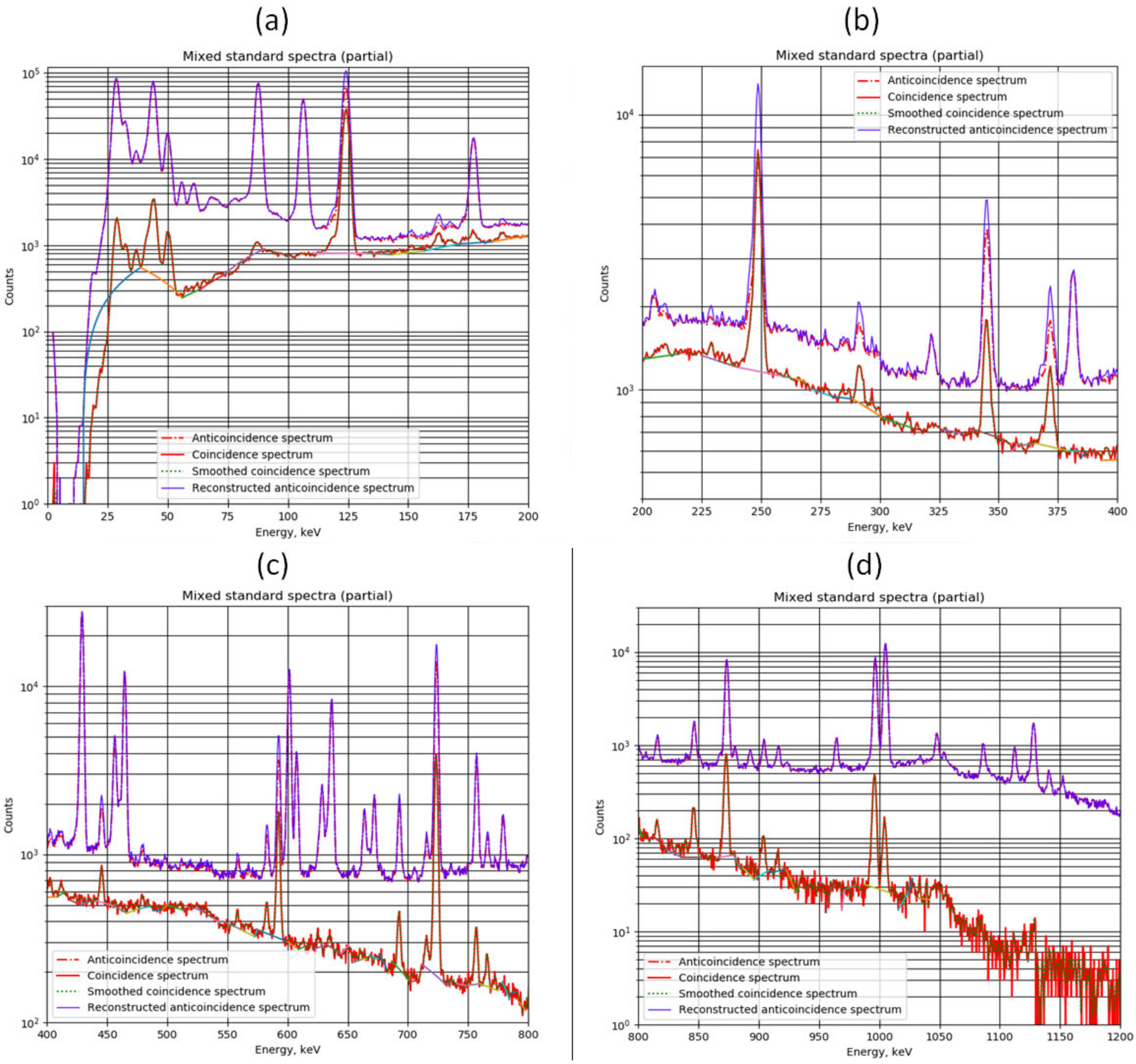

Figure 4: Comparison of anticoincidence, coincidence and reconstructed anticoincidence spectrum collected by the ^{125}Sb, ^{154}Eu and ^{155}Eu standard for the energy range 0-200 keV (a), 200-400 keV (b), 400-800 keV (c), 800-1200 keV (d)

radionuclides with cascade gamma emissions. The reconstructed anticoincidence spectrum therefore allows to determine a true efficiency curve per counting geometry and to estimate unbiased activity for the radionuclides with cascade decay scheme while maintaining the advantages of the anti-Compton spectrometer. As such, the software coupled with the digital list-mode data acquisition spectrometer expands the anti-Compton technique applications in environmental radioactivity analysis.

References

1. Weihua Zhang, Pawel Mekarski, Maxime Dion, Jing Yi, Kurt Ungar. A digital Compton suppression spectroscopy without gamma-ray coincidence-summing loss using list-mode multispectral data acquisition. J. Radioanal. Nucl. Chem. 2011. doi: 10.1007/s10967-011-1588-7.
2. ANS/IEEE Standard 325-1986. Test Procedures for Germanium Gamma Ray Detectors; 1986.
3. Weihua Zhang, Benjamin Keeshan, Pawel Mekarski, Jing Yi, Kurt Ungar. Performance evaluation and optimization for a newly developed digital list-mode data acquisition Compton suppression spectrometer. Applied Radiation and Isotopes. 2013; 81:96-102.
4. Savitzky A, Golay M. Smoothing and Differentiation of Data by Simplified Least Squares Procedure. Analytical Chemistry. 1964; 36:1627-1639.
5. Doletum Oy. Unisampo Advanced Gamma Spectrum Analysis Software, Version 1.98. User's Guide Espoo; 2003.
6. Baryon Oy. Shaman Expert System for Radionuclide Identification, Version 1.7. User's Guide. Espoo; 2003.
7. Plenteda R. A Monte Carlo Based Virtual Gamma Spectroscopy Laboratory. Ph.D. Thesis, Universitaetsbibliothek derTechnisch-enUniversitaet Wien, Resselgasse 4, A-1040 Wien, Austria, 118; 2002.